JOURNAL OF VIROLOGY, Nov. 2007, p. 12066–12070 Vol. 81, No. 21
0022-538X/07/$08.00+0 doi:10.1128/JVI.00818-07

Disease Duration Determines Canine Distemper Virus Neurovirulence▽

François Bonami, Penny A. Rudd, and Veronika von Messling*

INRS-Institut Armand-Frappier, University of Quebec, Laval, Quebec, Canada

Received 16 April 2007/Accepted 6 August 2007

The *Morbillivirus* hemagglutinin (H) protein mediates attachment to the target cell. To evaluate its contribution to canine distemper virus neurovirulence, we exchanged the H proteins of the wild-type strains 5804P and A75 and assessed the pathogenesis of the chimeric viruses in ferrets. Both strains are lethal to ferrets; however, 5804P causes a 2-week disease without neurological signs, whereas A75 is associated with a longer disease course and neurological involvement. We observed that both H proteins supported neuroinvasion and the subsequent development of clinical neurological signs if given enough time, demonstrating that disease duration is the main neurovirulence determinant.

Canine distemper virus (CDV), which infects a broad range of carnivores, is a close relative of the human pathogen measles virus (MV) (5). In its natural hosts, CDV reproduces all the signs of MV disease, including the characteristic rash, fever, respiratory and gastrointestinal involvement, and immunosuppression (16, 23). In addition, CDV displays one of the highest incidences of central nervous system (CNS) involvement within the *Morbillivirus* genus. During or after natural and experimental infections, about 30% of dogs exhibit neurological signs, but lesions are present in many more animals (17, 26). Ferrets are even more susceptible to CDV than dogs, and the lethality of wild-type strains reaches 100% (16, 23). When infected with a neurovirulent strain, most ferrets will develop neurological signs that increase with disease progression (4, 13).

The hemagglutinin (H) protein mediates viral particle attachment to the receptor on the target cell. With up to 10% variability among CDV strains, H is the least-conserved protein, and it determines in vitro tropism (9, 25). The role of the H protein in pathogenesis was initially investigated in rodent models of MV infection. The majority of mutations that accumulated during virus adaptation to growth in rodent brains map to the H protein (8), and introduction of these mutations into the parental strain replicated a neurovirulent phenotype (3, 15).

In ferrets, the wild-type strain 5804P leads to death within 2 weeks due to sepsis and multiorgan failure without neurological signs of disease (21). In contrast, the disease caused by the A75 strain usually lasts between 3 and 5 weeks, and most animals develop classical distemper-associated neurological signs, including chewing gum seizures and head pressing (13, 17). To evaluate the contribution of the H protein to these differences in neurological manifestation and disease duration, we exchanged the H genes in the two strains.

Chimeric viruses retain parental growth characteristics in vitro. The H proteins of the two strains (5804P and A75) are 2.8% divergent, consistent with the differences reported for unrelated strains (9, 19). The residues that vary are evenly distributed (Fig. 1A) and do not include amino acids interacting with the immune cell receptor SLAM (Fig. 1A, black bars) (20, 22). To assess the contribution of the H protein to the observed differences in pathogenesis, we produced two chimeric viruses: 5804P with the H gene of A75 (58/HA75) and A75 with the H gene of 5804P (A75/H58) (Fig. 1B). All viruses in this study express the enhanced green fluorescent protein (eGFP) protein from an additional transcription unit located between the H and polymerase genes. The viruses were recovered as described previously (25), and they displayed growth characteristics (Fig. 1C and D) and syncytium phenotypes (data not shown) similar to those of the parental strains in cell culture.

Disease duration determines the extent of CNS infection. The pathogenesis and neurovirulent potential of the chimeric viruses were assessed in ferrets, following protocols approved by the Institutional Animal Care and Use Committee of the INRS-Institut Armand Frappier. Intranasal inoculation with 10^5 50% tissue culture infectious doses ($TCID_{50}$) of the control parental viruses resulted in disease that was lethal within 2 weeks for virus strain 5804P and persisted for 3 to 6 weeks for virus strain A75 (Fig. 2A). Disease duration and clinical course correlated with the strain providing the genome backbone rather than the source of the H protein (Fig. 2A). One A75/H58-infected ferret experienced only a weak and short-lived viremia and survived the infection without developing any disease signs, which might have been due to residual maternal antibodies below detection levels. Immunological and virological parameters were assessed as described previously (24). The levels of cell-associated viremia and leukopenia caused by the different viruses were similar (Fig. 2B and C), but inhibition of lymphocyte proliferation upon phytohemagglutinin stimulation was less pronounced in A75-infected animals and significantly reduced in those inoculated with A75/H58 (Fig. 2D).

The A75 H protein facilitates neuroinvasion. We have shown that the olfactory bulb is the first site of macroscopically detectable infection in the CNS (13). We thus compared the extent of eGFP expression in the olfactory bulbs of animals infected with the parental and chimeric viruses. No eGFP expression was observed at 2 weeks in animals infected with

* Corresponding author. Mailing address: INRS-Institut Armand-Frappier, University of Quebec, 531, boul. des Prairies, Laval, Quebec H7V 1B7, Canada. Phone: (450) 687-5010. Fax: (450) 686-5305. E-mail: veronika.vonmessling@iaf.inrs.ca.

▽ Published ahead of print on 15 August 2007.

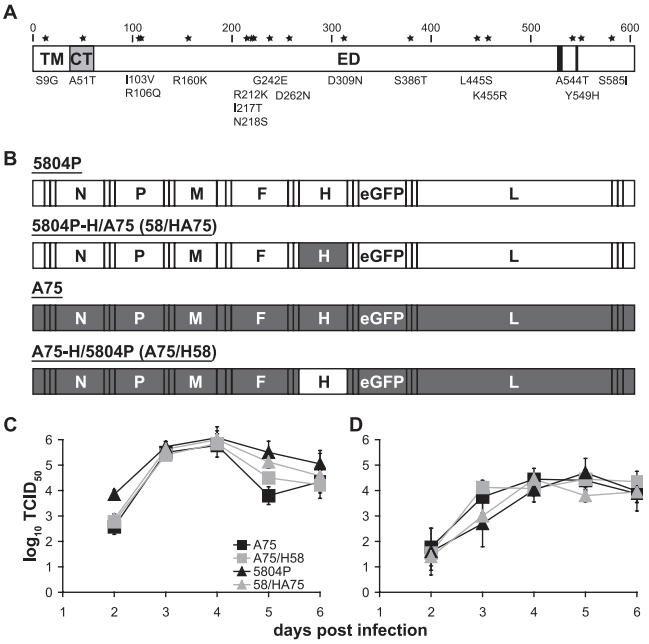

FIG. 1. Scheme and growth characteristics of the recombinant viruses produced. (A) Location of amino acids that vary between 5804P and A75 H proteins. The cytoplasmic tail (CT), transmembrane region (TM), and extracellular domain (ED) are represented by rectangles. SLAM-interacting residues (at positions 526 to 529 and 547 and 548) are represented by black bars. Amino acid numbers are indicated above the rectangles, and the locations of exchanged residues are marked by black stars. The A75 amino acid and its number within the protein, followed by the 5804P amino acid at that position, are noted below the rectangles. (B) Schemes of the parental and chimeric viruses. H genes were exchanged using the unique restriction sites BsrGI, located in the 3′ end of F gene, and AscI, positioned upstream of the eGFP start codon. A chimeric fragment combining the end of F and the FH untranslated region (UTR) from the recipient genome with the H open reading frame and the H-eGFP UTR from the donor strain by overlap extension PCR (6), and introduced into the recipient genome. Genetic material originating from 5804P is shown in white elongated boxes, while genetic material originating from A75 is represented by gray elongated boxes. Viral genes are represented by the letters N (nucleocapsid), P (phosphoprotein), M (matrix), F (fusion), and L (polymerase). The full names and abbreviated forms used throughout the article are indicated above the respective genome scheme. (C and D) Cell-associated virus (C) and free virus (D) production after infection of VerodogSLAMtag cells with a multiplicity of infection of 0.01. Virus titers were determined by 50% endpoint dilution at the indicated times after infection with a limit of virus detection at 1.7 50% $TCID_{50}$. Viruses in the A75 genomic context are represented by squares, while viruses in the 5804P genomic context are represented by triangles. Parental strains are shown in black, and recombinant viruses in gray. Values indicate the averages of at least three experiments, and error bars represent standard deviations.

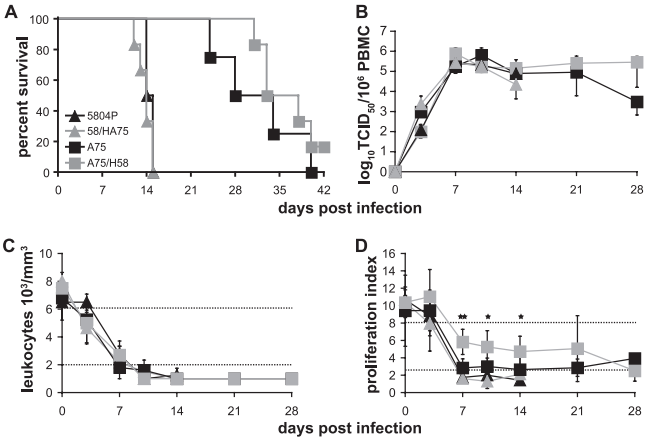

FIG. 2. Comparison of survival and immunological parameters of parental and chimeric viruses. (A) Survival curves of animals infected with parental strains 5804P and A75 ($n = 4$) and chimeric viruses 58/HA75 and A75/H58 ($n = 6$). Viruses in the A75 genomic context are represented by squares, while viruses in the 5804P genomic context are represented by triangles. Parental strains are shown in black, and recombinant viruses in gray. (B to D) Cell-associated CDV titer per million peripheral blood mononuclear cells (PBMC) (B), leukocyte number (C), and in vitro proliferation activity (D) of animals inoculated with the different viruses. Days after infection are plotted on the *x* axes, and the 50% $TCID_{50}$ per million PBMC, leukocyte number, or proliferation index is indicated on the *y* axis. Leukocyte numbers were determined directly from whole blood using the Unopette system (BD Biosciences). PBMC were isolated by Ficoll gradient centrifugation. Proliferation activity is expressed as a ratio of 5-bromo-2′-deoxyuridine incorporation of PBMC either stimulated with 100 μg/ml phytohemagglutinin or left untreated. The top dotted lines represent the threshold level for normal values, while the bottom dotted lines separate moderate and severe immunosuppression. Error bars indicate standard deviations. Two stars represent a *P* value of <0.005, one star indicates *P* values of <0.05. *P* values were calculated by comparing 5804P- and A75/H58-infected groups at the indicated time points with an unpaired, two-tailed Student *t* test.

5804P or viruses of A75 genomic origin (Fig. 3A). However, the presence of the A75 H protein resulted in clearly detectable eGFP expression in five out of the six animals infected (Fig. 3A, 58/HA75). No H-protein-mediated differences in infection levels were noted at the time of death for A75 viruses (Fig. 3B, compare top and bottom panels).

Histological analysis of sagittal olfactory bulb cryosections revealed few infected foci for virus strain 5804P (Fig. 3C), indicating that the macroscopically observed difference was quantitative rather than qualitative. A large number of infected olfactory glomeruli were detected in sections of 58/HA75-infected animals, confirming the macroscopically observed extent of infection (Fig. 3C). Consistent with our macroscopic results, the level of infection in olfactory bulbs from A75- and A75/H58-inoculated animals was similar (Fig. 3C, compare top and bottom right panels). In contrast, when comparing the infection in the choroid plexus, which is an important site of hematogenous neuroinvasion, we found similar amounts of infected cells in sections from animals sacrificed at similar time points (Fig. 3D, compare top and bottom panels).

We then compared the macroscopic distribution of eGFP expression throughout the brains of animals infected with A75 or A75/H58. The infection was predominantly concentrated in the olfactory bulb, the rostral region of the frontal lobe, and the brain stem, regardless of the H protein present (data not shown). Confocal microscopy analysis of cryosections stained with the respective cellular markers revealed that most of the infected cells in the macroscopically identified regions were either neurons (Fig. 4A and C) or glial cells (Fig. 4B and D), as described previously for A75 (13).

Despite their differences in clinical neurological presentation, all strains established a microscopically detectable infec-

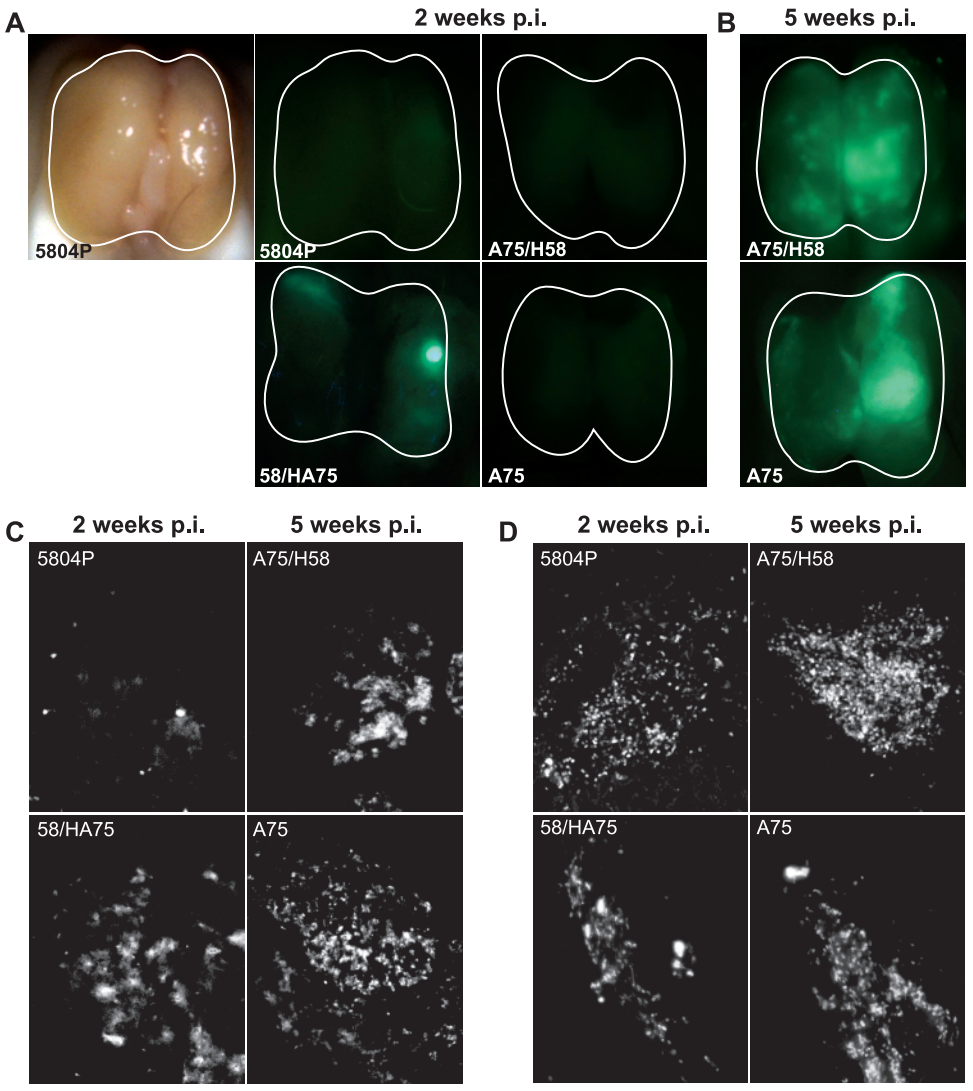

FIG. 3. Macroscopic and microscopic visualization of CNS infection. (A and B) Macroscopic imaging of the olfactory bulbs. The contours of the individual olfactory bulbs are outlined by a white line. Normal light photograph of the olfactory bulb originating from a 5804P-infected animal, and photographs of the same organ from animals infected with the parental and chimeric viruses after eGFP fluorescence excitation using the Macro-Illumination imaging system (Lightools, Encinitas, CA). The name of the respective virus is indicated on the picture. Pictures were taken at 2 weeks postinfection (p.i.) for all viruses (A) and at 5 weeks for A75 and A75/H58 (B). (C and D) Microscopic analysis of CNS infection. Ten- to 15-μm sagittal cryosections of paraformaldehyde-perfused and fixed brains were analyzed for eGFP expression at a magnification of ×200. Representative regions of olfactory bulbs (C) and choroid plexus (D) photographed at the time of death, 2 weeks after infection for 5804P and 58/HA75, and 5 weeks for A75 and A75/H58, are shown.

tion in the choroid plexus and the olfactory bulb and are thus neuroinvasive. Furthermore, introduction of the 5804P H protein into the A75 background resulted in disease duration and neurovirulence similar to those of the parental A75 strain, demonstrating that the 5804P H protein is able to mediate CNS invasion if given sufficient time. The lack of neurological signs in 5804P-infected animals might therefore be due to its rapid disease progression in other organs, rather than the virus' inability to infect CNS cells. The similar levels of cell-associated viremia and leukopenia indicate that it is a qualitative rather than quantitative difference determining disease duration. These findings, in combination with the observed variation in lymphocyte proliferation inhibition, point towards a difference in immunosuppression as the underlying cause. In vitro studies and experiments in rodent models have shown that contact between the H protein and immune cells is essential to induce proliferation inhibition (11, 14). Our chimeric viruses, in which H proteins were exchanged between two lethal strains, provide the first evidence that viral proteins other than H modulate the severity of this inhibition, thereby influencing disease duration and ultimately outcome.

The CDV H protein determines viral tropism and thus the potential target cells and tissues within the infected organism (3, 7, 20). We have observed the A75 H protein facilitates neuroinvasion in the 5804P genomic context without altering disease duration. This is consistent with the observation that the transfer of the H protein originating from a rodent brain-adapted MV strain into the vaccine virus conferred neuroin-

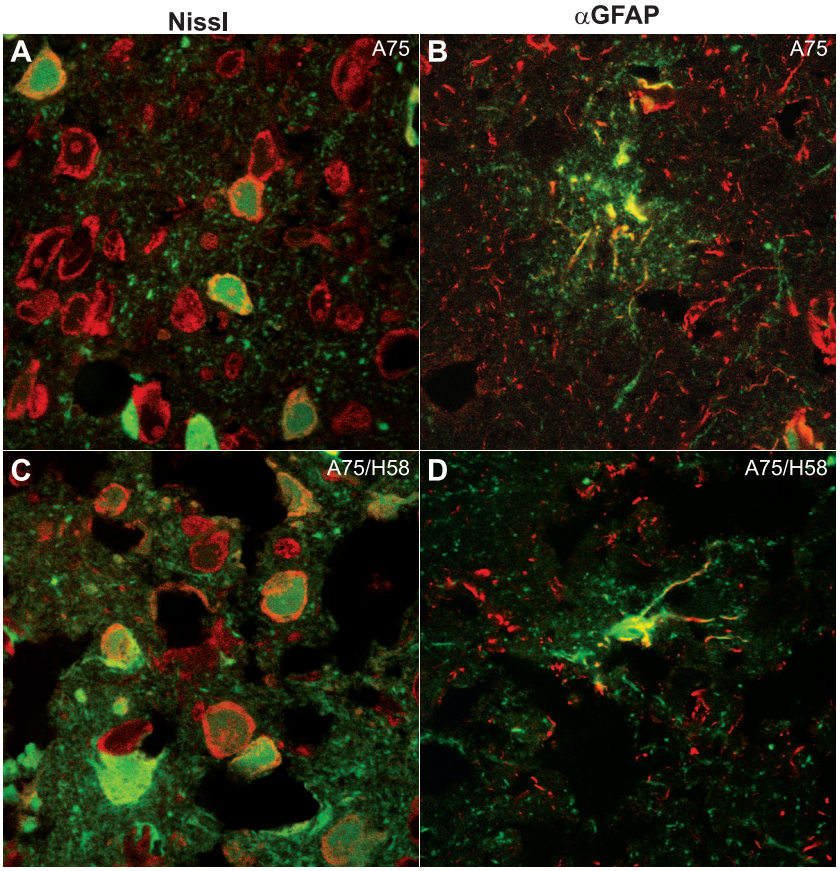

FIG. 4. Microscopic identification of target cells of viruses with A75 backbone. (A and C) Infected neurons; (B and D) glial cells. Infected cells are detected by eGFP expression, and neurons and glial cells are visualized with the 530/615 NeuroTrace Nissl stain (Nissl) and a rabbit anti-glial fibrillary acidic protein polyclonal antiserum (αGFAP), respectively, and an Alexa Fluor 568-labeled secondary antibody. Yellow staining and red and green staining of the same cell represent infected cells positive for the respective cellular marker. Shown are composite images of confocal microscopy analyses of cryosections at a magnification of ×1,000 of an A75-infected brain in the top panels and of an A75/H58-infected brain in the bottom panels.

vasive properties but failed to reproduce the extent of CNS dissemination seen with the parental strain (3, 15). Taken together, these findings indicate that H proteins from neurovirulent strains are more efficient at mediating neuron infection, probably due to an increased affinity for the yet to be identified receptor on these cells.

Ferrets infected with wild-type CDV are unable to mount an effective antiviral immune response (18) and thus provide us with a unique insight into the full spectrum of *Morbillivirus* disease. Inoculation with the highly virulent strain 5804P results in rapidly progressing disease characterized by the complete loss of immune system function, impaired mucosal membrane integrity, and death, similar to rinderpest virus in cattle (1, 2). The course of A75 represents an intermediate scenario where, despite widespread infection of immune and epithelial tissues, residual immune function seems to be maintained, resulting in prolonged survival and CNS invasion, consistent with the course of MV in severely immunodeficient individuals (10, 12). Finally, sublethal viruses, which mirror the course and signs of an uncomplicated MV infection in humans (5), do not cause CNS involvement, and the immune system is able to overcome its infection-induced suppression sufficiently to control and eliminate the virus (21). This dynamic interplay between the virus and the host's immune system, and the resulting differences in the duration of the infection observed in our CDV model, might also explain the variety of CNS diseases associated with MV.

We thank Roberto Cattaneo and Christoph Springfeld for helpful comments on the manuscript. We are also thankful to all laboratory members for continuing support and lively discussions.

This work was supported by CIHR operating funds (MOP-66989) and salary support to V.V.M. and an Armand-Frappier Foundation scholarship to P.R.

REFERENCES

1. **Banyard, A. C., M. D. Baron, and T. Barrett.** 2005. A role for virus promoters in determining the pathogenesis of *Rinderpest virus* in cattle. J. Gen. Virol. **86:**1083–1092.
2. **Brown, D. D., B. K. Rima, I. V. Allen, M. D. Baron, A. C. Banyard, T. Barrett, and W. P. Duprex.** 2005. Rational attenuation of a morbillivirus by modulating the activity of the RNA-dependent RNA polymerase. J. Virol. **79:** 14330–14338.
3. **Duprex, W. P., I. Duffy, S. McQuaid, L. Hamill, S. L. Cosby, M. A. Billeter, J. Schneider-Schaulies, V. ter Meulen, and B. K. Rima.** 1999. The H gene of rodent brain-adapted measles virus confers neurovirulence to the Edmonston vaccine strain. J. Virol. **73:**6916–6922.
4. **Evermann, J. F., C. W. Leathers, J. R. Gorham, A. J. McKeirnan, and M. J. Appel.** 2001. Pathogenesis of two strains of lion (Panthera leo) morbillivirus in ferrets (Mustela putorius furo). Vet. Pathol. **38:**311–316.
5. **Griffin, D. E.** 2001. Measles virus, p. 1401–1441. *In* D. M. Knipe and P. M.

Howley (ed.), Fields virology, 4th ed., vol. 1. Lippincott Williams & Wilkins, Philadelphia, PA.
6. **Ho, S. N., H. D. Hunt, R. M. Horton, J. K. Pullen, and L. R. Pease.** 1989. Site-directed mutagenesis by overlap extension using the polymerase chain reaction. Gene **77:**51–59.
7. **Johnston, I. C., V. ter Meulen, J. Schneider-Schaulies, and S. Schneider-Schaulies.** 1999. A recombinant measles vaccine virus expressing wild-type glycoproteins: consequences for viral spread and cell tropism. J. Virol. **73:** 6903–6915.
8. **Liebert, U. G., S. G. Flanagan, S. Loffler, K. Baczko, V. ter Meulen, and B. K. Rima.** 1994. Antigenic determinants of measles virus hemagglutinin associated with neurovirulence. J. Virol. **68:**1486–1493.
9. **Martella, V., F. Cirone, G. Elia, E. Lorusso, N. Decaro, M. Campolo, C. Desario, M. S. Lucente, A. L. Bellacicco, M. Blixenkrone-Moller, L. E. Carmichael, and C. Buonavoglia.** 2006. Heterogeneity within the hemagglutinin genes of canine distemper virus (CDV) strains detected in Italy. Vet. Microbiol. **116:**301–309.
10. **McQuaid, S., S. L. Cosby, K. Koffi, M. Honde, J. Kirk, and S. B. Lucas.** 1998. Distribution of measles virus in the central nervous system of HIV-seropositive children. Acta Neuropathol. (Berlin) **96:**637–642.
11. **Ohgimoto, S., K. Ohgimoto, S. Niewiesk, I. M. Klagge, J. Pfeuffer, I. C. Johnston, J. Schneider-Schaulies, A. Weidmann, V. ter Meulen, and S. Schneider-Schaulies.** 2001. The haemagglutinin protein is an important determinant of measles virus tropism for dendritic cells in vitro. J. Gen. Virol. **82:**1835–1844.
12. **Plaza, J. A., and G. J. Nuovo.** 2005. Histologic and molecular correlates of fatal measles infection in children. Diagn. Mol. Pathol. **14:**97–102.
13. **Rudd, P. A., R. Cattaneo, and V. von Messling.** 2006. Canine distemper virus uses both the anterograde and the hematogenous pathway for neuroinvasion. J. Virol. **80:**9361–9370.
14. **Schlender, J., J. J. Schnorr, P. Spielhoffer, T. Cathomen, R. Cattaneo, M. A. Billeter, V. ter Meulen, and S. Schneider-Schaulies.** 1996. Interaction of measles virus glycoproteins with the surface of uninfected peripheral blood lymphocytes induces immunosuppression in vitro. Proc. Natl. Acad. Sci. USA **93:**13194–13199.
15. **Schubert, S., K. Moller-Ehrlich, K. Singethan, S. Wiese, W. P. Duprex, B. K. Rima, S. Niewiesk, and J. Schneider-Schaulies.** 2006. A mouse model of persistent brain infection with recombinant *Measles virus*. J. Gen. Virol. **87:**2011–2019.
16. **Stephensen, C. B., J. Welter, S. R. Thaker, J. Taylor, J. Tartaglia, and E. Paoletti.** 1997. Canine distemper virus (CDV) infection of ferrets as a model for testing *Morbillivirus* vaccine strategies: NYVAC- and ALVAC-based CDV recombinants protect against symptomatic infection. J. Virol. **71:**1506–1513.
17. **Summers, B. A., H. A. Greisen, and M. J. Appel.** 1984. Canine distemper encephalomyelitis: variation with virus strain. J. Comp. Pathol. **94:**65–75.
18. **Svitek, N., and V. von Messling.** 2007. Early cytokine mRNA profiles predict Morbillivirus disease outcome in ferrets. Virology **362:**404–410.
19. **Takeda, M., T. Sakaguchi, Y. Li, F. Kobune, A. Kato, and Y. Nagai.** 1999. The genome nucleotide sequence of a contemporary wild strain of measles virus and its comparison with the classical Edmonston strain genome. Virology **256:**340–350.
20. **Vongpunsawad, S., N. Oezgun, W. Braun, and R. Cattaneo.** 2004. Selectively receptor-blind measles viruses: identification of residues necessary for SLAM- or CD46-induced fusion and their localization on a new hemagglutinin structural model. J. Virol. **78:**302–313.
21. **von Messling, V., D. Milosevic, and R. Cattaneo.** 2004. Tropism illuminated: lymphocyte-based pathways blazed by lethal morbillivirus through the host immune system. Proc. Natl. Acad. Sci. USA **101:**14216–14221.
22. **von Messling, V., N. Oezguen, Q. Zheng, S. Vongpunsawad, W. Braun, and R. Cattaneo.** 2005. Nearby clusters of hemagglutinin residues sustain SLAM-dependent canine distemper virus entry in peripheral blood mononuclear cells. J. Virol. **79:**5857–5862.
23. **von Messling, V., C. Springfeld, P. Devaux, and R. Cattaneo.** 2003. A ferret model of canine distemper virus virulence and immunosuppression. J. Virol. **77:**12579–12591.
24. **von Messling, V., N. Svitek, and R. Cattaneo.** 2006. Receptor (SLAM [CD150]) recognition and the V protein sustain swift lymphocyte-based invasion of mucosal tissue and lymphatic organs by a morbillivirus. J. Virol. **80:**6084–6092.
25. **von Messling, V., G. Zimmer, G. Herrler, L. Haas, and R. Cattaneo.** 2001. The hemagglutinin of canine distemper virus determines tropism and cytopathogenicity. J. Virol. **75:**6418–6427.
26. **Winters, K. A., L. E. Mathes, S. Krakowka, and R. G. Olsen.** 1983. Immunoglobulin class response to canine distemper virus in gnotobiotic dogs. Vet. Immunol. Immunopathol. **5:**209–215.